

Standardization of Split Hopkinson Pressure Bar Compression System without Frictional Effects for Metal Plate Specimens*

Yasuhisa SATO**, Minoru YAMASHITA***, Toshio HATTORI***
and Syota SUZUKI**

**Faculty of Engineering, Tohoku Gakuin University,
1-13-1 Chuo, Tagajo 985-8537, Japan

E-mail: ysato@tjcc.tohoku-gakuin.ac.jp

***Faculty of Engineering, Gifu University,
1-1 Yanagido, Gifu 501-1193, Japan

E-mail: minoruy@gifu-u.ac.jp

Abstract

The effects of variables, such as the dimensions of a test specimen and the friction between the plate specimen and the tools, on the average stress measured in the usual split Hopkinson-Davies pressure bar (SHPB) compression test are estimated, and a method, which is a variant of the well-known Cook and Larke extrapolation method, is established for a constant-strain-rate test using some tapered striker bars to determine the curves of dynamic resistance to homogeneous deformation, i.e., the intrinsic stress-strain curves, by trial and error. The research involves the SHPB compression tests on metal specimens with four or five initial ratios of diameter to height and an analysis of the resulting curves. It is shown that the friction coefficient for various conditions is somewhat complicated and hence it is difficult to estimate the friction coefficient by the SHPB compression test. Then we formulate an extrapolation method to reduce friction to a minimum for the SHPB compression test at a constant strain rate: approximately 1000 [1/s] for metal plate specimens. We conclude that this kind of SHPB system with a constant-strain-rate test followed by the extrapolation procedure is a standard SHPB compression system for metal plate specimens.

Key words: SHPB Compression System, Plate Metal Specimen, Constant Strain Rate Test, Friction Coefficient, Extrapolation Method, Standard SHPB Test, Aluminum, Copper, Brass, Steel

1. Introduction

Since Kolsky⁽¹⁾ first described in detail the use of the split Hopkinson-Davies pressure bar (SHPB) system for determining the dynamic mechanical properties of materials, Campbell and Duby⁽²⁾, Hauser et al.⁽³⁾, Lindholm⁽⁴⁾, Tanaka et al.⁽⁵⁾, and many others have used the SHPB method applying bonded strain gauges. However, the accuracy of the stress-strain curves obtained by the SHPB method was limited by the accuracy of the oscilloscopes, until we used, in ca. 1978, a digital wave memory with an A/D converter at high speed, e.g., 1 Msample/s, such as that produced by Kawasaki Electronica Co. Ltd. Because of the rapid progress in IT over the last three decades, the time and amplitudes of output signals can be correctly estimated. Furthermore, the methods of data reduction can now be performed quickly on personal computers and associated peripheral equipment. On

*Received 14 Oct., 2008 (No. 08-0722)
[DOI: 10.1299/jmmp.3.584]

the other hand, Bertholf and Karnes⁽⁶⁾ presented the results of the first comprehensive two-dimensional numerical analysis of the technique, and quantitatively described the effects of realistic friction and of variations in both the specimen geometry and the imposed strain rate on the validity of the assumptions used in analyzing experimental data. They also showed that, as seen in Figs. 11 and 12 in their paper, even a friction coefficient of 0.05 produced approximately a ten percent variation in the axial stress as well as a ten percent deviation from a one-dimensional stress state for the diameter-to-height ratio, $d/h = 3.3$; therefore friction between the specimen and the elastic bars considerably affects the response of the specimen.

In the present study, friction coefficients under various conditions of friction in the dynamic compression tests using the ordinary and constant-strain-rate SHPB systems were estimated quantitatively. However, the values of these friction coefficients were random. Then, extrapolation was carried out in the SHPB compression test⁽⁷⁻⁹⁾ coupled with a constant-strain-rate test⁽¹⁰⁻¹²⁾ for four kinds of metal plate specimens. Extrapolation of the experimental line between average stress and the diameter-to-height ratio (d/h) back to a zero value of d/h appears to be reasonably safe, and should give the intrinsic stress for the parameter strain. The complete stress-strain curve can be constructed in this manner from the results of three or four compression tests on specimens with different d/h ratios (preferably in a wide range for greater accuracy).

2. Experimental and Tentative Analysis

2.1 Relationship between average pressure and current ratio of diameter-to-height^(7,8)

The friction between the specimen and the tools causes the pressure on these surfaces to be distributed nonuniformly and also leads to inhomogeneous deformation in the specimen. Therefore, the uniaxial stress-strain curve cannot be obtained directly from the measurement, even after a long time from the start of dynamic compression, because the effect of friction cannot be eliminated in practice after the effect of inertia force fades out.

Let a cylindrical specimen have the initial diameter d_0 and height h_0 , and at any arbitrary time, let its diameter and height become d and h . Denoting the deformation energy of the specimen by W_i , the external force by f , the axial velocity by v , and the incident and transmitter sides of the specimen by subscripts 1 and 2 (see Fig. 1), we have

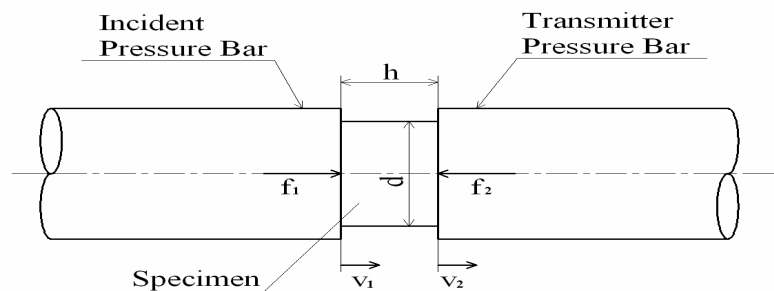


Fig. 1 Configuration of specimen in SHPB test

$$\dot{W}_i + \dot{W}_f + \dot{W}_k = f_1 v_1 - f_2 v_2, \quad (1)$$

where W_f is the friction loss and W_k is the kinetic energy of the specimen. These are defined by

$$\dot{W}_f = 2\pi \int_0^{d/2} \mu(p_1 + p_2) r v_r dr, \quad (2)$$

$$\dot{W}_k = \rho_0 \int_V (\dot{v} v + v_r \dot{v}_r) dV, \quad (3)$$

where μ is Amontons' friction coefficient, p is the pressure on the end face, v_r is the radial velocity, and V and ρ_0 are the volume and the density, respectively, of the specimen.

When the effect of friction is absent or negligible, the specimen approaches the uniaxially uniform state after a short period $\tau_o^{(7)}$. Thus, the force f_1 approximately equals f_2 . Then \dot{W}_i is given by

$$\dot{W}_i \approx \sigma \dot{\varepsilon} V, \quad (4)$$

where σ is the true stress in compression and $\dot{\varepsilon}$ is the average strain rate defined by

$$\dot{\varepsilon} = \frac{v_1 - v_2}{h}. \quad (5)$$

Assuming that there is no volume change, the radial velocity at a point r on the specimen is

$$v_r \approx (v_1 - v_2) \frac{r}{2h} = \frac{1}{2} r \dot{\varepsilon}. \quad (6)$$

Substitution of the velocity, Eq. (6), into Eq. (2) and Eq. (3) yields

$$\dot{W}_f \approx 2\pi \dot{\varepsilon} \int_0^{d/2} \mu p_1 r^2 dr, \quad (7)$$

$$\dot{W}_k \approx \rho_0 \left\{ \left(\frac{h^2}{12} + \frac{d^2}{32} \right) \ddot{\varepsilon} + \left(\frac{h^2}{12} - \frac{d^2}{64} \right) \dot{\varepsilon}^2 \right\} \dot{\varepsilon} V, \quad (8)$$

where $\ddot{\varepsilon}$ is the rate of $\dot{\varepsilon}$ and a linear relationship between the axial velocity and the axial co-ordinate is assumed. This expression is the same as that derived by Samanta⁽¹³⁾. It

will be shown later for our experiments presented here that \dot{W}_k of Eq. (1) can be neglected.

Although μ and p_1 are dependent upon r , the integral can be expressed, owing to the mean value theorem, by

$$\int_0^{d/2} \mu p_1 r^2 dr = \bar{\mu} \sigma \int_0^{d/2} r^2 dr = \frac{1}{24} \bar{\mu} \sigma d^3, \quad (9)$$

where $\bar{\mu}$ is a constant depending on the friction between the specimen and the pressure bars.

When $\mu d/h$ is not too large, $\bar{\mu}$ coincides with μ used by Siebel, who assumed that μ is independent of r , and the distribution of pressure is given by⁽¹⁴⁾

$$p_1 = \sigma \exp \{ 2\mu(d/2 - r)/h \}. \quad (10)$$

We designate $\bar{\mu}$ as the friction coefficient hereafter without ().

From Eq. (1), Eq. (4) and Eq. (7) - (9),

$$\bar{p} \approx \sigma + \frac{\mu d}{3h} \sigma + \rho_0 \left\{ \left(\frac{h^2}{12} + \frac{d^2}{32} \right) \ddot{\varepsilon} + \left(\frac{h^2}{12} - \frac{d^2}{64} \right) \dot{\varepsilon}^2 \right\}, \quad (11)$$

where $\bar{p} = f_1 / (\frac{\pi}{4} d^2)$. The absolute value of the last term is estimated to be less than

0.3 MPa, except during the initial rising part of the stress pulse [see Fig. 12 in Ref. (7)].

This is relatively small compared with the average pressure \bar{p} and can be neglected. Then

we obtain the relationship between \bar{p} and σ , namely:

$$\bar{p} \approx \left(1 + \frac{\mu d}{3h} \right) \sigma. \quad (12)$$

From Eq. (12) the relationship between the average nominal stress $\bar{\sigma}_N$ and the nominal

stress σ_N obtained in case of no friction, at the current compressive strain is

$$\overline{\sigma_N} \approx \left(1 + \frac{\mu d}{3h}\right) \sigma_N, \quad (13)$$

where $\overline{\sigma_N} = f_1 / \left(\frac{\pi}{4} d_0^2\right)$.

Since $\overline{\mu}$ is equal to μ used by Siebel as described above, the results of this analysis agree with those of his analysis of the relationship between the applied average pressure \overline{p} and the current flow stress σ under quasi-static compression⁽¹⁴⁾. This linearity of the relationship between \overline{p} and d/h in Eq. (12) for specimens with the same work hardening has been observed experimentally for copper cylinders subjected to quasi-static compression by Cook and Larke over a d/h range from 1 to 3 [see for Ref. (14)]; their results correspond to a value of μ between 0.2 and 0.3⁽¹⁴⁾. Thus, even for $\mu=0.3$ under a rather unfavorable condition of lubrication, Eq. (12) or Eq. (13) may be a good approximation for cylindrical specimens.

2.2 Friction coefficient under various conditions in SHPB compression test

2.2.1 How to determine coefficient of friction

Because a linear relationship, Eq. (12), between the average pressure and the diameter-to-height ratio is obtained by a least squares method using experimental data, the friction coefficient μ can be determined using the linear equation (12) as follows:

$$\overline{p} = \sigma + (\mu \sigma / 3) \frac{d}{h} = \sigma + s \frac{d}{h}, \quad (14)$$

where the slope s is equal to $\mu \sigma / 3$. Then, there exists the following relationship of the friction coefficient

$$\mu = 3s / \sigma. \quad (15)$$

Therefore, we can determine friction coefficient μ for given parameter ε using Eq. (15).

2.2.2 SHPB test of A1050P-0 for four kinds of lubricants

The loading pulse in the incident pressure bar of 1200 mm length is initiated by axial impact from a striker bar of 300 or 280 mm length accelerated to the impact velocity using rubber bands, as shown in Fig. 2. By applying the one-dimensional elastic-wave-propagation theory, we can determine the particle velocity, displacement and force at both faces of the specimen as functions of time from the stress-time characteristics of the incident stress pulse, σ_I , the reflected stress pulse, σ_R , and the transmitted stress pulse, σ_T ,

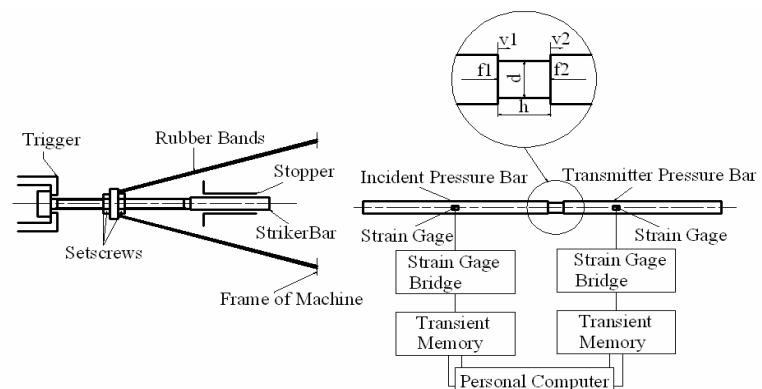


Fig.2 Schematic diagram of the SHPB compression system

which is measured in the transmitter pressure bar of 800 mm length. We require the following relations.

Velocities:

$$v_1(t) = \frac{C_b}{E_b} \{ \sigma_I(t) - \sigma_R(t) \}, \quad v_2(t) = \frac{C_b}{E_b} \sigma_T(t). \quad (16)$$

Displacements:

$$u_1(t) = \int_0^t v_1(t') dt', \quad u_2(t) = \int_0^t v_2(t') dt'. \quad (17)$$

Forces:

$$F_1(t) = A_b \{ \sigma_I(t) + \sigma_R(t) \}, \quad F_2(t) = A_b \sigma_T(t). \quad (18)$$

The incident and transmitted sides of the specimen are denoted by 1 and 2, respectively, the origin of the time scale t is taken to be the instant the specimen begins to be compressed, and E_b , C_b and A_b are Young's modulus, the wave velocity and the cross-sectional area of the pressure bars, respectively. The average strain rate, strain and stress in the specimen are given by

$$\dot{\varepsilon}(t) = \frac{v_1 - v_2}{h_0} = \frac{C_b}{h_0 E_b} \{ \sigma_I(t) - \sigma_R(t) - \sigma_T(t) \}, \quad (19)$$

$$\varepsilon(t) = \frac{u_1 - u_2}{h_0} = \frac{C_b}{h_0 E_b} \int_0^t \{ \sigma_I(t') - \sigma_R(t') - \sigma_T(t') \} dt', \quad (20)$$

$$\sigma(t) = \frac{F_1 + F_2}{2A_0} = \frac{A_b}{2A_0} \{ \sigma_I(t) + \sigma_R(t) + \sigma_T(t) \}, \quad (21)$$

where the positive values of stress and strain in the specimen stand for compression, and h_0 and A_0 are the initial height and the cross-sectional area of the specimen, respectively.

The following approximate expressions are obtained, assuming equivalent forces at the two ends of metallic specimens⁽¹⁵⁾:

$$A_b \{ \sigma_I(t) + \sigma_R(t) \} = F_1(t) \approx F_2(t) = A_b \sigma_T(t). \quad (22)$$

With this approximation, the strain rate $\dot{\varepsilon}$ and stress σ in the specimen are proportional to the reflected pulse σ_R and transmitted pulse σ_T , respectively, thus

$$\dot{\varepsilon}(t) \approx -\frac{2C_b}{h_0 E_b} \sigma_R(t), \quad (23)$$

$$\varepsilon(t) \approx -\frac{2C_b}{h_0 E_b} \int_0^t \sigma_R(t') dt', \quad (24)$$

$$\sigma(t) \approx \frac{A_b}{A_0} \sigma_T(t). \quad (25)$$

To determine friction coefficients for four kinds of lubricants in a SHPB compression test of A1050P-0, we used an A1050P aluminium plate (JIS-H4000; JIS means Japanese Industrial Standard) 20 mm thick, 1000 mm wide and 2000 mm long, from which a series of cylinders of various dimensions were machined. SHPB compression of the aluminium cylinders of different dimensions, which are given in Table 1, was carried out on a SUS304 stainless steel bar (JIS-G4303) finished by centerless grinding (JIS-G4318) (h7). The faces in contact with the specimen were ground flat. The diameters of the pressure bar, which are also shown in Table 1, are slightly larger than those of the specimen. The end faces of the specimen were made parallel by prestraining them by a few tenths of a percent using a set of compression jigs.

Then the specimens were annealed at 623 K for one hour in an electric furnace. The

effect of friction between the specimen and the pressure bars was investigated under the four different friction conditions given in Table 2.

Table 1. Dimensions of aluminium cylinders and diameters of pressure bars used in SHPB compression tests of these specimens.

Diameter of pressure bar, mm		5.0	15.0	20.0
Specimen	Diameter (d_0), mm	4.74	14.23	18.97
	Height (h_0), mm	$\frac{5.0}{[0.95]}$	$\frac{5.0}{[2.85]}$	$\frac{5.0}{[3.79]}$
	$[d_0/h_0]$	$\frac{10.0}{[0.47]}$	—	$\frac{10.0}{[1.90]}$

Table 2. Lubricants

Lubricant	Remarks
Mineral oil	Kinematic viscosity $20 \times 10^{-6} \text{ m}^2/\text{s}$ (293K)
Grease	Lithium base; multipurpose type
Teflon	PTFE film, $50 \mu \text{ m}$ thick
None	Dry condition

Table 3. Heat treatment conditions and hardness for four kinds of sheet metal specimens.

Material [JIS]	Dimensions of specimen	Annealing	Hardness [JIS (HV)]
A1050P-0 [H4000]	Diameter = 18 mm Thickness = 1 mm	In air; 623 K; 3600 s	19.6
C1100P-0 [H3100]	Diameter = 18 mm Thickness = 1 mm	In N_2 gas; 823 K; 3600 s	40.4
C2801P-0 [H3100]	Diameter = 18 mm Thickness = 1 mm	In N_2 gas; 823 K; 3600 s	102.4
SPCC-A [G3141]	Diameter = 18 mm Thickness = 1 mm	In vacuum; 1183K; 1800s	106.8

2.2.3 SHPB test using grease for four kinds of plate metal specimens

Friction coefficients in the SHPB test are determined for four kinds of annealed sheet metals: aluminium (A1050P-0: JIS-H4000), copper (C1100P-0: JIS-H3100), brass (C2801P-0: JIS-H3100) and steel (SPCC-A: JIS-G3141). Table 3 shows the conditions of heat treatment and Vickers hardness for these specimens.

Although the friction coefficient estimation using Eq. (15) with SHPB test data is

somewhat complicated, the complete stress-strain curve can be constructed by using an extrapolation of the results of three or four compression tests on specimens with different d/h ratios (preferably in a wide range for greater accuracy).

2.3 Extrapolation method in SHPB compression test for four kinds of specimens

Dynamic compression of four kinds of circular sheet metals, which are given in Table 3, are carried out on cemented carbide bars: G6 of the WC-Co system (manufactured by Sumitomo Electric Industries, Ltd.) finished by centerless grinding. The faces in contact with the specimens are also ground flat. We use this kind of hard metal bar as the Hopkinson pressure bar, since such hard specimens as steel and brass are to be tested.

For the extrapolation method, we perform four SHPB compression tests on each kind of metal specimen with four d/h ratios. The initial diameter is 18 mm, and the initial heights are 1, 2, 3 and 4 mm. The heights of 2, 3 and 4 mm are those of laminated specimens composed of two, three and four pieces of the same sheet metal, respectively. Then, specimens with the four different initial d_0/h_0 ratios are used for each of the four metals.

2.4 Constant strain rate loading in SHPB compression test

Generally, the flow stress of a specimen is considered to be a function of strain, strain rate, and equivalent friction $\mu d/h$. Therefore, it is desirable that each of three or four compression tests on specimens with different d/h ratios under conditions of constant-strain-rate loading in the SHPB compression test. Thus, we must prepare striker bars of various cross sections or tapered cylindrical bars in order to maintain the constant strain rate or to realize the reflected pulse with the constant amplitude in the SHPB test⁽¹⁰⁻¹²⁾. For the sake of simplicity, we use the nine tapered gauge bars shown in Fig. 3 as striker bars and change the impact velocity of the striker bar against the incident bar; therefore, we maintained the constant strain rate of 10^3 s^{-1} in aluminium and copper specimens with four d_0/h_0 ratios. However, we maintained the constant strain rate of 800 s^{-1} in the harder brass specimen with four d_0/h_0 ratios. For the hardest steel specimen with four d_0/h_0 ratios, we conducted the test at the mean strain rate of 10^3 s^{-1} by using the straight cemented carbide striker bar, since the cemented carbide striker gauge bar set is very costly.

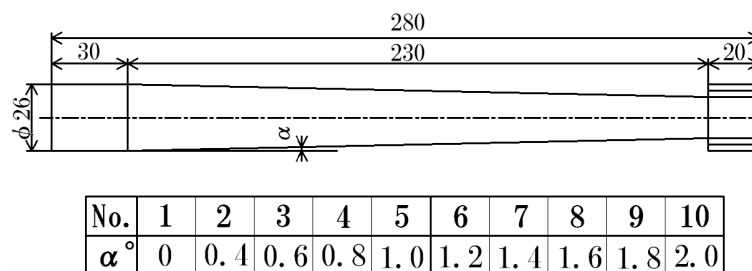


Fig. 3 Tapered striker bar with solid sleeve bearing for the constant-strain-rate SHPB test. After these tapered bars (alloy tool steel: SKD61: JIS-G4404) were finished in a lathe, they were treated by heating (air hardening: JIS-G3106)

3. Results and discussion

3.1 Friction coefficient for four lubricants in SHPB test of A1050P-0

Fig. 4 shows a comparison of friction coefficients at low and high strain rates for various lubricants for annealed commercially pure aluminium (A1050P-0). Details of the specimens and the pressure bars in the SHPB system are given in Table 1, and details of the four lubricants are given in Table 2. Friction coefficient μ is determined using Eq. (15) on the basis of the linear relationship between average stress and the diameter-to-height ratio.

In Fig. 4, we can see that for small strain, $\epsilon_n \leq 0.01$, μ at a high strain rate is larger

than μ at a low strain rate. However, when ε_n becomes larger to approximately 0.05, μ for all lubricants at high strain rate decreases, and yet, μ for all lubricants at low strain rate increases. Fig. 4 indicates that grease exhibits the best performance among all lubricants examined here. On the other hand, μ of PTFE or grease for small strain of approximately 0.01-0.03 at low strain rate becomes negative. The reason for the negative μ of PTFE is as follows: since PTFE is softer than the specimen, after the commencement of compression, the portion of the specimen in contact with PTFE is drawn outwards by the generated friction force. Thus we conclude that grease is the best in the four lubrication conditions. Hereafter, we use grease as the lubricant throughout this study.

3.2 Friction coefficient of grease in SHPB test for four kinds of plate metal specimens

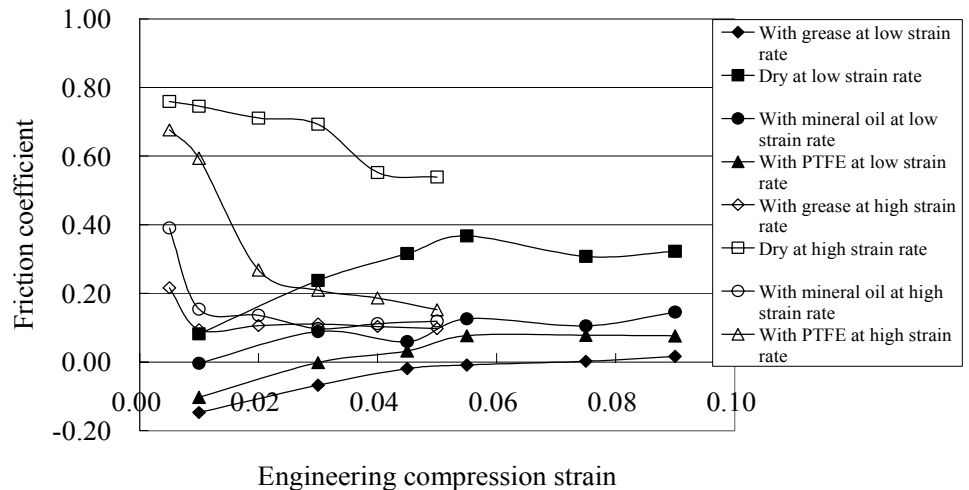


Fig. 4 Effects of friction coefficients μ on compressive strain ε_n at low (approximately 10^{-3} s^{-1}) and high (approximately 600 s^{-1}) strain rates for various lubricants (mineral oil, grease, Teflon and none); A1050P-0 specimens

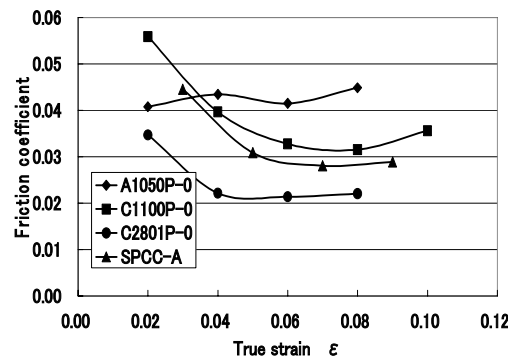


Fig.5 Effects of strain on friction coefficient at strain rate of approximately 1000 s^{-1}

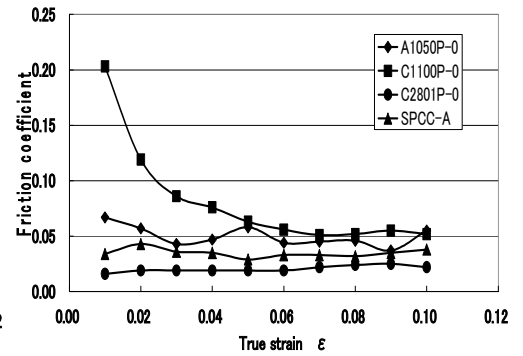


Fig.6 Effects of strain on friction coefficient at strain rate of approximately 0.2 s^{-1}

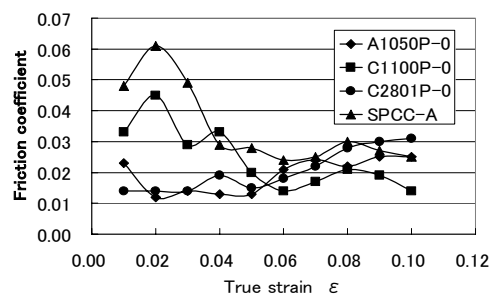


Fig.7 Effects of strain on friction coefficient at strain rate of approximately 0.04 s^{-1}

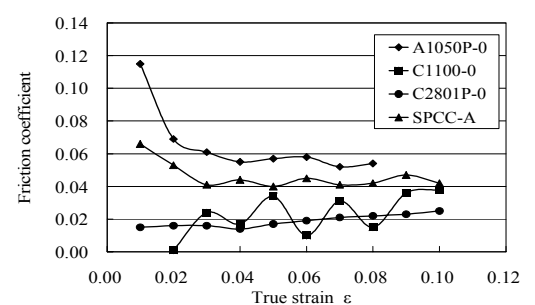


Fig.8 Effects of strain on friction coefficient at strain rate of 0.0002 s^{-1}

Figs. 5 and 6 show the effects of strain on the friction coefficient for the four kinds of sheet metals at the strain rates of approximately 10^3 s^{-1} and 0.2 s^{-1} , respectively, where stress and strain are used as true stress and strain, respectively. Hereafter, these are defined as follows:

$$\sigma = \sigma_N(1 - \varepsilon_N), \quad \varepsilon = -\ln(1 - \varepsilon_N),$$

where σ_N and ε_N are the nominal stress and nominal strain, respectively.

Figs. 7 and 8 show the effects of strain on the friction coefficient for the four kinds of sheet metals at the strain rates of approximately 0.04 s^{-1} and 0.0002 s^{-1} , respectively.

It is observed that the friction coefficients μ are not large as those shown in Figs. 5~8. e.g., $\mu \leq 0.05$, but it is difficult or somewhat complicated to measure the value of μ during each SHPB or low-strain-rate test. We consider that the best compression test without the frictional effects is the extrapolation method from the results of three or four compression tests on specimens with different d_0/h_0 ratios.

3.3 Mean stress vs strain curves of A1050P-0 at constant strain rate of 1000 s^{-1}

Fig. 9 shows the mean true stress versus true strain of aluminium (A1050P-0) with four initial diameter/height (d_0/h_0) ratios. Although the mean true stress containing friction effects are plotted against the true strain, only true stress is designated on the ordinate. The number of laminated plates of a specimen is shown in Fig.9. Fig.10 shows the strain rate versus strain corresponding to each strain for the same d_0/h_0 ratio in Fig.9, respectively.

It is demonstrated that four kinds of the tapered striker bar having the shape of a frusta of a cone selected, respectively, by a trial and error method from the nine tapered gauge bars shown in Fig.3 enables an almost constant strain rate, for example, 1000 s^{-1} , during the test throughout the deformation of the aluminium specimen with four d_0/h_0 ratios, corresponding to the tapered striker bar at a suitable impact velocity, as shown in Fig.10.

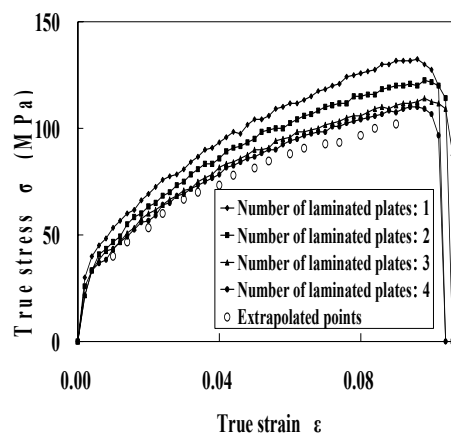


Fig.9 Mean stress-strain curves of A1050P-0 for various numbers of plates⁽¹⁶⁾

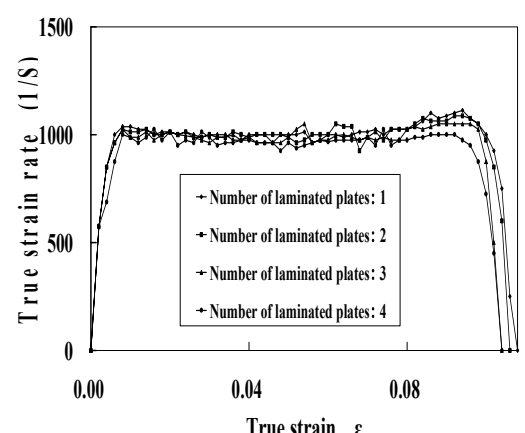


Fig.10 Strain rate vs strain curves equivalent to the curves in Fig.9, respectively⁽¹⁶⁾

3.4 Extrapolated stress-strain relationships of A1050P-0

The stress-strain relationships under the conditions of uniaxial stress are determined by the extrapolation procedure of data in Fig. 9 derived from the conventional SHPB test for aluminium. Fig. 11 shows that the relationship between the mean stress and diameter/height (d/h) ratio for various values of strain, for A1050P-0 lubricated with grease, can be expressed by Eq. (12). Then the intrinsic stress-strain curves drawn in Fig. 12 show the extrapolated stress vs strain curves of A1050P-0 at various constant strain rates.

3.5 Extrapolated stress-strain relationships of C1100P-0

The stress-strain curves under conditions of uniaxial stress for C1100P-0 are also determined by the extrapolation method, similarly to A1050P-0. Fig. 13 shows that the rela-

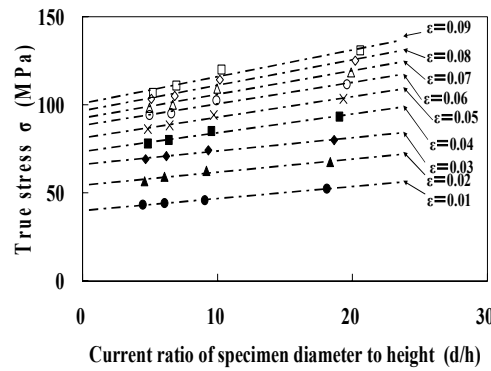


Fig.11 Relationship between mean stress and d/h ratio for various values of strain for A1050P-0 lubricated with grease at constant strain rate of 10^3 s^{-1} ⁽¹⁶⁾

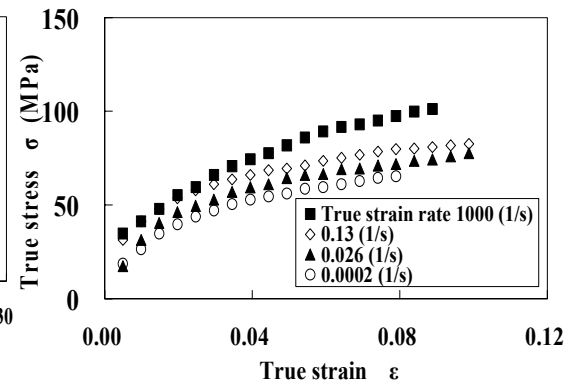


Fig.12 Extrapolated stress vs strain curves of A1050P-0 at various constant strain rates under conditions of uniaxial stress ⁽¹⁶⁾

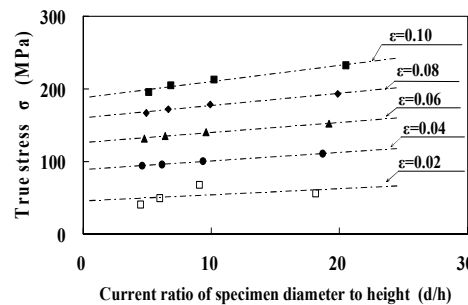


Fig.13 Relationship between mean stress and d/h ratio for various values of strain for C1100P-0 lubricated with grease at 10^3 s^{-1} ⁽¹⁶⁾

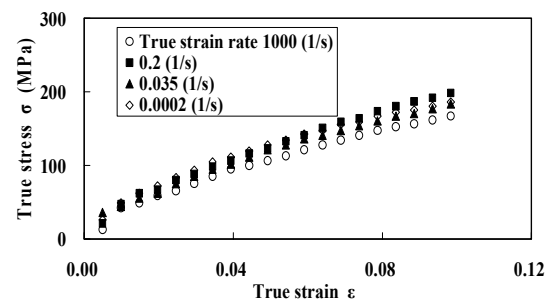


Fig.14 Extrapolated stress vs strain curves for C1100P-0 at various constant strain rates under conditions of uniaxial stress ⁽¹⁶⁾

tionship between the mean stress and d/h ratio for various values of strain for copper lubricated with grease can be expressed by the linear Eq. (12). Then the intrinsic stress-strain curves can be derived under the constant strain rate of 1000 s^{-1} . The intrinsic stress vs strain curves drawn in Fig. 14 show the extrapolated stress vs strain curves for copper at various strain rates.

3.6 Extrapolated stress-strain relationships of C2801P-0

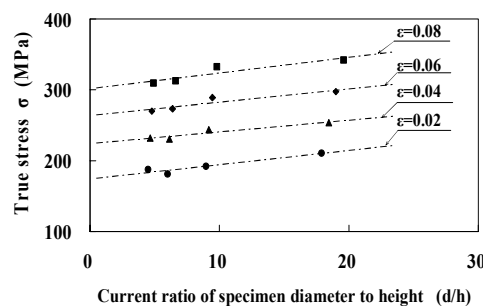


Fig.15 Relationship between mean stress and d/h ratio for various values of strain for C2801P-0 lubricated with grease at 800 s^{-1} ⁽¹⁶⁾

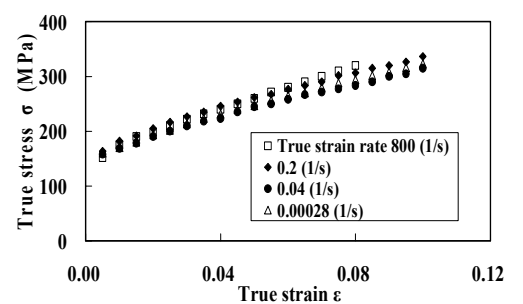


Fig.16 Extrapolated stress vs strain curves of C2801P-0 at various constant strain rates under conditions of uniaxial stress ⁽¹⁶⁾

The stress-strain curves under conditions of uniaxial stress for brass are determined by the extrapolation procedure of the mean stress-strain curves derived from the conventional

SHPB test. Fig. 15 shows that the relationship between the mean stress and d/h ratio for various values of strain for brass (C2801P-0) lubricated with grease can be expressed by Eq. (12). Then the intrinsic stress-strain curves can be derived under the constant high strain rate of 800 s^{-1} . The intrinsic stress-strain curves drawn on Fig. 16 show the extrapolated stress vs strain curves of C2801P-0 at various constant strain rates.

3.7 Extrapolated stress-strain relationships of SPCC-A

The stress-strain curves of steel (SPCC-A) under the conditions of uniaxial stress are also derived from the extrapolation procedure of the mean stress-strain curves determined by the conventional SHPB test for SPCC-A. Fig. 17 shows that the relationship between the mean stress and d/h ratio for various values of strain for steel lubricated with grease can be expressed by Eq. (12). Then the intrinsic stress-strain relationships can be derived under the average high strain rate of 1000 s^{-1} . The intrinsic stress-strain curves drawn on Fig. 18 show the extrapolated stress vs strain curves of steel at various strain rates.

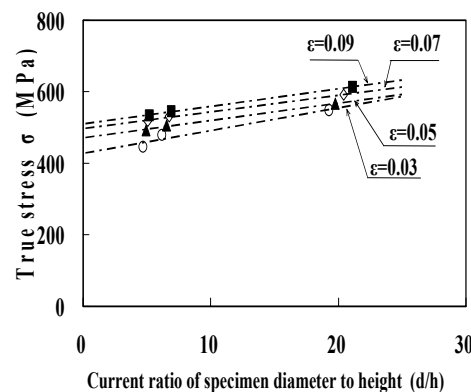


Fig.17 Relationship between mean stress and d/h ratio for various values of strain for SPCC-A lubricated with grease at strain rate of approximately 1000 s^{-1} ⁽¹⁶⁾

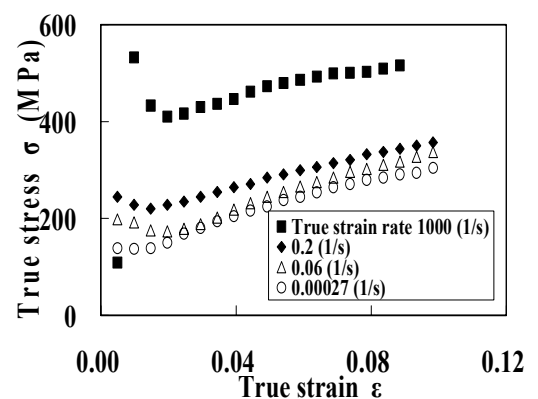


Fig.18 Extrapolated stress vs strain curves of SPCC-A at various strain rates under conditions of uniaxial stress⁽¹⁶⁾

3.8 Discussions

(1) Bertholf and Karnes⁽⁶⁾ demonstrated, as described in the introduction of this paper, that even a friction coefficient of 0.05 produced an approximately ten percent variation in axial stress as well as a ten percent derivation from the one-dimensional stress state for $d/h=3.3$; therefore, friction between the specimen and the elastic bars considerably affects the response of the specimen. However, it is not easy to determine the friction coefficient in the SHPB compression test. Hence, by using the extrapolation method, we showed that the intrinsic stress-strain curve can be constructed from the results of four compression tests on metal plate specimens with four different d/h ratios at the high strain rate using the SHPB system and at low strain rates using the Instron testing system.

(2) Lindholm described, in his paper⁽⁴⁾ on the SHPB compression test, that theoretically, it would be possible to maintain a constant strain rate in the specimen by varying the loading pulse shape, but practically, this does not seem feasible. On the other hand, we were able to maintain constant strain rate in aluminium, copper and brass specimens in the SHPB compression test using four or five kinds of tapered striker bars, machined using a lathe, as gauge bars. It is necessary to control the strain rate of each specimen with a different d/h ratio to determine the intrinsic stress-strain relationships of such plate specimens as aluminium, copper, brass and steel plates.

4. Concluding remarks

We recommend the following method for a standardized SHPB compression test. We used a tapered striker gauge set to carry out, by trial and error, the constant-strain-rate SHPB compression tests followed by extrapolation procedures to derive the intrinsic stress-strain relationships at high strain rates for metallic materials containing sheet metals.

The precise accuracy of the experimental results should be estimated on the basis of a standard two-dimensional axisymmetric numerical analysis of these tests. A standard numerical simulator for each kind of impact material tester will be necessary in the near future.

References

- (1) Kolsky, H., An investigation of the mechanical properties of materials at very high rates of loading, *Proc. Phys. Soc.*, Vol. B26 (1949), pp. 676-700.
- (2) Campbell, J. D. and Duby, J., The yield behavior of mild steel in dynamic compression, *Proc. Phys. Soc. London*, Vol. A236, No. 1204 (1956), pp. 24-40.
- (3) Hauser, F. E., Simmons, J. A. and Dorn, J. E., Strain rate effects in plastic wave propagation, *Response of metals to high velocity deformation*, (1960), pp. 93-110, Interscience Publishers.
- (4) Lindholm, U. S., Some experiments with the split Hopkinson pressure bar, *J. Mech. Phys. Solids*, Vol. 12 (1964), pp. 317-335.
- (5) Tanaka, K., Kinoshita, M. and Matsuo, T., Compressive deformation of aluminium at high strain rate, *Proc. 7th Japan Congr. Test. Mat.*, (1964), pp. 91-93.
- (6) Bertholf, L. D. and Karnes, C. H., Two-dimensional analysis of the split Hopkinson pressure bar system, *J. Mech. Phys. Solids*, Vol. 23 (1975), pp.1-19.
- (7) Sato, Y. and Takeyama, H., An extrapolation method for obtaining stress-strain curves at high rates of strain in uniaxial compression, *Tech. Rep. of Tohoku Univ.*, Vol. 44, No. 2 (1979), pp. 287-302.
- (8) Sato, Y. and Takeyama, H., An extrapolation method for obtaining stress-strain curves at high rates of strain in uniaxial compression - The elimination of the frictional effect on the flow stress in a high speed compression testing I -, *J. of JSTP (in Japanese)*, Vol. 22, No. 249 (1981), pp. 1023-1029.
- (9) Sato, Y. and Takeyama, H., An application of the extrapolation method to high-strain-rate compression testing of aluminum and its accuracy - The elimination of the frictional effect on the flow stress in a high speed compression testing II -, *J. of JSTP (in Japanese)*, Vol. 22, No. 251(1981), pp. 1236-1243.
- (10) Sato, Y. and Takeyama, H., The use of the split Hopkinson pressure bar to obtain dynamic stress-strain data at constant strain rates (part I), *Tech. Rep. of Tohoku Univ.*, Vol. 43, No. 2 (1978), pp. 303-315.
- (11) Sato, Y. and Takeyama, H., The use of the split Hopkinson pressure bar to deform a metal specimen at a predetermined strain rate history - A constant strain rate testing using the compression SHPB system I -, *J. of JSTP (in Japanese)*, Vol. 23, No. 254 (1982), pp. 252-258.
- (12) Sato, Y. and Takeyama, H., On the striker bars with variable cross-sectional areas for the constant strain-rate compression testing - A constant strain-rate testing using the compression SHPB system II -, *J. of JSTP (in Japanese)*, Vol. 24, No. 270 (1983), pp. 744-750.
- (13) Samanta, S. K., Dynamic deformation of aluminium and copper at elevated temperatures, *J. Mech. Phys. Solids*, Vol. 19 (1971), pp. 117-135.
- (14) Hill, R., *The Mathematical Theory of Plasticity*, (1950), pp. 277-278, Clarendon Press.
- (15) Sato, Y., *Dissertation*, Tohoku University, (1973), pp. 238-239.
- (16) Sato, Y. and Yamashita, M., On Standardization of SHPB compression test, *ICTP2008*, (2008), pp. 1813-1820, ISBN 978-89-5708-152-5, Korea.